Thermal Management Modeling for Thermal Runaway Avoidance in Lithium-ion Batteries

Nicolas F. Ponchaut, Ph.D., P.E.
Managing Engineer

Francesco Colella, Ph.D.
Sr. Associate

Vijay Somandepalli, Ph.D., P.E.
Managing Engineer

Michael Stern, Ph.D.
Associate

Exponent Inc.
Natick, MA

Abstract

The development of lithium-ion battery technology have made it possible to store and use large amounts of electrical energy in applications such as microgrids and off-grid electrical storage. However, the safety aspects of using these large energy storage battery packs have received less attention. For example, an unintentional sudden release of energy through a thermal runaway event can occur and can be destructive. Developing thermal management systems for upset conditions in battery packs requires a clear understanding of the heat generation mechanisms and kinetics associated with the failures mechanisms of lithium-ion batteries.

Despite the efforts to avoid thermal runaway situations, upset and unforeseen conditions can arise where a cell or a pack would reach a sufficiently high temperature to initiate exothermic reactions that often are initially slow to develop. Such situations can be the result of a rapid cell discharge, of cell defects, or of a change in ambient conditions. Properly designed thermal management systems should be able to lower pack temperatures, effectively slowing down or stopping these exothermic reactions. On the other hand, a poorly designed system can let the temperature rise to a point where a thermal runaway becomes inevitable.

In this work, we will describe a framework for assessing the efficacy of thermal management systems. To investigate heating phenomena of the cell due to inherent internal resistance, cells were discharged at various rates and their internal impedance was measured. In addition, to investigate the self-heating behavior of cells due to the slow exothermic reactions that are typically the precursor to a thermal runaway event, cells were tested in an Accelerated Rate Calorimeter (ARC). Using these test data, discharge and self-heating were included in a Computational Fluid Dynamics (CFD) model of a lithium-ion cell pack. The CFD model was then used to quantify the effect of an enclosure around a multi-cell pack system as well as the efficacy of aluminum fins.

This model and framework can be applied to the design and optimization of pack size systems, including the cells and the associated thermal management system. These tools allow rapid simulation and analyses of various thermal upset conditions in cells, modules and packs to assess the efficacy of a system design in avoiding thermal runaway.

Introduction

The emergence of Lithium ion (Li-ion) battery technologies has made the storage of large amounts of energy efficiently a reality. From a technological standpoint, Li-ion battery technologies are an attractive option for stationary power storage applications like microgrids and off-grid electrical storage because of their high energy density as well as their rechargeable nature. However, from a safety and fire protection standpoint, a high energy density coupled with a flammable organic, rather than aqueous, electrolyte has created a number of new challenges with regard to the design and use of batteries containing Li-ion cells, and with regard to the storage and handling of these batteries. Historically, there have been reports of incidents of fire and explosion hazards resulting from Li-ion batteries, ranging from consumer electronic devices such as cellular phones, and laptops, and more recently, incidents have also been reported for electric vehicles and other transportation systems.

Thermal hazards from Li-ion battery failures can be the result of various failure modes such as overcharging of the cells, mechanical crush, penetration of foreign objects, excessive cell discharge rate and external thermal stresses. Because Li-ion cell chemistries have an inherent high energy density, a cell failure can generate significant amounts of heat capable of combusting other cell components leading to an intense fire event. An energetic failure of Li-ion cells and batteries that releases significant amounts of heat and other flammable material is called a thermal runaway. Another hazard can result from a breach in the cell packaging (before or after a thermal event), which can allow flammable electrolyte vapors to permeate and fill available space, creating a possible flash fire or explosion risk. Additionally, the degradation and reaction products of a thermal runaway event in a lithium-ion cell and a battery pack can create potentially combustible gases which pose similar or more powerful explosion risks to that of the un-combusted flammable electrolyte.

For large power packs, such as those used in power-storage applications, the number of cells and batteries that can become involved in a thermal runaway event increases because of the high packing density of these cells and batteries and the propensity of the thermal runaway events to cascade to neighboring cells and batteries. Li-ion cells also generate heat internally when they are charged and discharged in normal use. In the absence of an appropriate effective heat removal system, the temperatures within the cells and batteries can reach limits where an upset condition such as thermal runaway becomes likely. As a result, special attention has to be paid to protecting the batteries from conditions that can lead to thermal runaway and to prevent heat from accumulating within the cells and battery packs. In practice, these conditions are achieved by using various thermal management solutions that utilize various heat removal and temperature control strategies to maintain these cells and battery packs at optimal thermal conditions.

Typical thermal managements systems use the forced motion of a fluid such as air or water to remove heat from regions that generate heat. The rate of heat removal in such systems is dependent upon the rate of fluid flow and the heat transfer properties of the fluid. To correctly size and optimize a thermal management system, the system can be modeled in Computational Fluid Dynamics (CFD). In the present work, Exponent proposes such a model which is able to model the thermal management system, along with the effect of cell discharge rates, external thermal stresses and exothermic reactions precursor to thermal runaway event.

The Lithium-Ion Battery

Lithium-ion batteries are a type of rechargeable, or secondary, battery.[1] Lithium-ion batteries are widely deployed in consumer electronics and are increasingly being considered for larger applications, such as electric vehicles. Lithium-ion batteries often possess higher energy storage than most other types of rechargeable batteries, which means that they can be smaller and lighter for a given application. They also have very low self-discharge rates and therefore last longer when not in use.

The lithium-ion battery is composed primarily of three parts: the positive electrode, the electrolyte filled separator, and the negative electrode. Current collectors are placed against each electrode, and represent where the external circuit is connected. During charging, lithium ions migrate from the positive electrode to the negative electrode; the reverse occurs during discharging. The batteries are designed such that the lithium ions have a much greater affinity for the positive electrode than the negative electrode; therefore, energy can be extracted from the battery when lithium ions are allowed to migrate from the negative electrode to the positive electrode. A representative diagram of a lithium-ion battery can be seen in Figure 1.

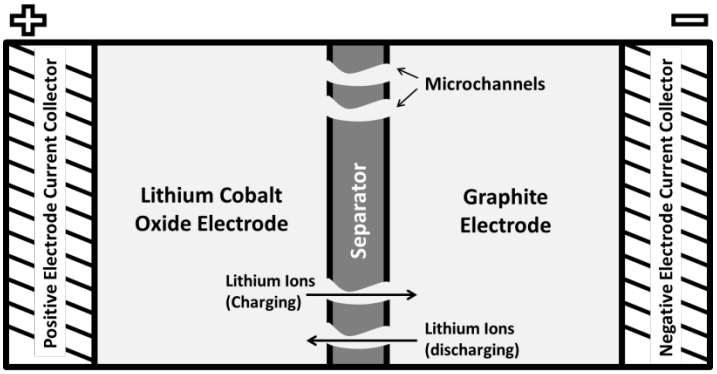

Figure 1 - Schematic diagram of a lithium-ion battery with a $LiCoO_2$ positive electrode.

Graphite is widely used as the negative electrode in lithium ion batteries. The separator is commonly a porous polyolefin material such as polyethylene, polypropylene, or a blend of both. The separator is impregnated with an electrolyte solution consisting of an organic solvent and lithium salt. Common solvents include carbonates, such as ethylene carbonate and diethyl carbonate. Lithium hexafluorophosphate ($LiPF_6$) is a common lithium salt used in Li-ion electrolytes. Significant research and development efforts have been expended to find an optimal positive electrode material which provides a large voltage and high stability.[2] Unfortunately, stability and energy content are intrinsically competitive, and materials which provide higher voltages, like lithium cobalt dioxide ($LiCoO_2$), also present higher safety concerns.[3] Safety is a general concern for all lithium ion batteries since they all use combustible electrolytes as opposed to the aqueous electrolytes found in alkaline, lead-acid, and nickel-metal hydride batteries.

Accelerating Rate Calorimetry

Accelerating Rate Calorimetry (ARC) is used to monitor the temperature evolution of a battery under adiabatic conditions.[4] The battery is placed in a chamber that mimics the temperature on the surface of the battery, *i.e.* if the battery begins to self-heat, the oven will match the temperature rise. The temperature in the chamber is slowly increased until the battery exceeds a threshold rate of self-heating. Once the threshold is exceeded, the chamber mimics the battery temperature as it rises until the battery runs out of energy or reaches an end temperature.

In practice, no battery would operate in a truly adiabatic environment; however, a battery in the center of a large uncooled pack or a battery surrounded by significant insulation could experience a nearly adiabatic environment. The ARC simulates a worst case scenario and measures the minimum temperature required to experience a thermal runaway event.

Figure 2 shows rate of temperature rise of a fully charged $LiCoO_2$ pouch battery during an ARC experiment after the threshold self-heating rate of 0.01°C/min has been exceeded. The battery weighed 23 grams and was rated for 3.7 V with 2100 mAh of capacity. At temperatures below 80°C, the self-heating rate is small, but as the temperature increases beyond 115°C, the self-heating rate increases dramatically as does the possibility of a thermal runaway. At 180°C the heating rate of the cell has become uncontrollable (the battery heating more than 15°C per minute). Shortly thereafter, the cell short-circuits, which leads to a rapid increase in temperature and venting of the pressurized gases. The ARC results demonstrate the consequences that occur when batteries are allowed to overheat and undergo a thermal runaway process.

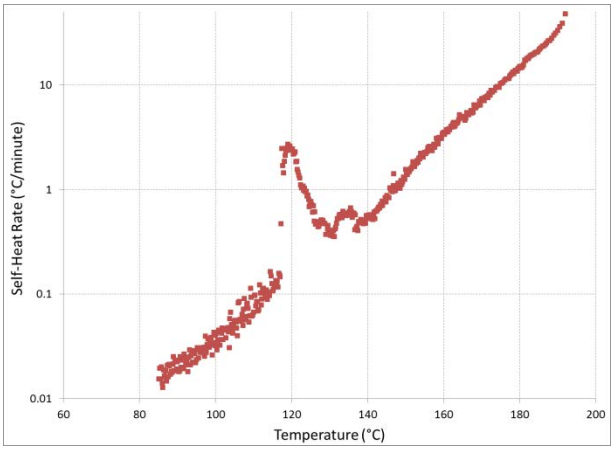

Figure 2 - Self-heating rate versus temperature of cell at 100% SOC during exotherm.

Thermal model

The experimental results were used as input conditions for a series of case studies comparing multiple design options for a battery module thermal management system. The battery module investigated consists of twenty 20 Ah Li-ion pouch cells. The module contains 21 aluminum plates with fins sandwiched between them. Multiple cooling layouts were considered:

- **Layout 1:** No forced convection, the fins are surrounded with air
- **Layout 2:** Cooling system with forced flow of air at 1 m/s
- **Layout 3:** Cooling system with forced flow of air at 2 m/s
- **Layout 4:** Cooling system with forced flow of water at 0.5 m/s

In all the layouts, the thermal contact resistance between the cooling fins and the pouch cell is assumed to be negligible (perfect thermal contact). The battery module is considered to be enclosed in a plastic casing leaving an approximate 1 cm air gap around the module. Layouts 2 to 4 include a forced convection cooling system that is located above the battery module. The cooling (air or water) channel is designed in order to allow the cooling fluid to flow along the aluminum fins. The computational model simulates both the heat transfer in the solid media (fins and battery) as well as the fluid-dynamics in the air gaps around the cells and in the cooling channels. Figure 3 shows two three-dimensional views of the battery module layout considered in this paper. The pouch-cells and the cooling fins are represented in light grey and orange, respectively (see Figure 3.a). Figure 3.b shows the air gaps between the battery module and the exterior casing. The blue region represents the air gap around the cells where natural convection heat transfer occurs. The green area located above the cells represents the channels where the cooling fluid is flowing.

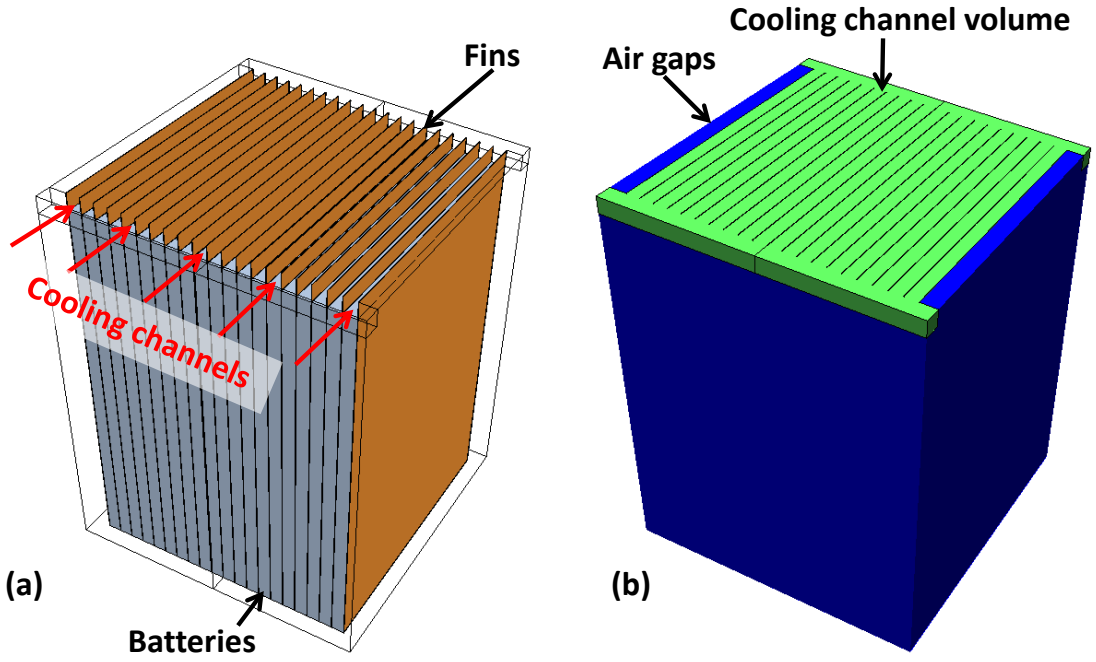

Figure 3 – Three dimensional representation of the lithium-ion battery module layouts considered in this study.

The main operating characteristics of each pouch cell are summarized in Table 1.

Table 1: Main battery cell specifications	
Cell type	Lithium-ion Polymer Cell, wound construction
Nominal Capacity [Ah]	19.6
Nominal voltage [V]	3.7
Dimensions [in]	6.5 × 9 × 5/16

The time dependent analysis of the thermal behavior of the battery module required the characterization of average properties of the pouch cells and the cooling fins. In particular, given the multilayered structure of the cell, two different thermal conductivities were used for the directions in and out of the cell plane: the in-plane conductivity k_{ip} is equal to 24.8 W/m-K; the out-of-plane conductivity k_{op} is equal to 1.0 W/m-K.[5] The cell average density and specific heat capacity were calculated based on the cell composition and using a volume weighted average as follows.

$$\rho_c c_{p,c} = \frac{\sum \rho_i c_{p,i} V_i}{V} \qquad (1)$$

where ρ_c is the average cell density, $c_{p,c}$ is the average cell specific heat capacity and V is the total cell volume. The density, specific heat capacity and volume of each of the cell components are ρ_i, $c_{p,i}$, and V_i, respectively. For simplicity, only the major components of the cell were considered for the evaluation of the average thermal properties. Table 2 summarizes the composition and thermal properties of each of the battery main components.

Table 2: battery composition and thermal properties[5]			
Component	**% (by mass)**	**Density [kg/m^3]**	**Heat capacity [J/kg-K]**
Separator	6.87%	1008.98	1978.16
Al Cathode ($LiCoO_2$ coated)	45.50%	2328.50	1269.21
Cu Anode (Graphite coated)	37.45%	1347.33	1473.4
Electrolyte	10.18%	1129.95	2055.1

The resulting cell average thermal capacity $\rho_c c_{p,c}$ is equal to 2335 kJ/m^3-K. The average thermal capacity of the aluminum fin is equal to 2360 kJ/m^3-K.[6]

Two internal heat generation mechanisms were considered in the thermal model:

- Heat generation due to normal operating conditions, *i.e.* heat generated during cell discharge (q)
- Heat generation due to exothermic chemical reactions (q_{sh})

The heat-generation rate during normal operation (q) was calculated by using the cell current and the cell resistance (assumed equal to 3mΩ). The rate of heat generation per unit volume due to self-heating (q_{sh}) has been extrapolated from the ARC testing results despite the difference between the tested and the simulated cell capacity. This assumption is deemed valid as the cell chemistry is the main parameter that controls the rate of self-heating as a function of temperature.

Figure 4 displays the temperature dependent self-heating curve as obtained from the experiments and implemented in the thermal model. The results show that the self-heating contribution is negligible at temperatures below 80°C and peaks at a temperature of approximately 120°C.

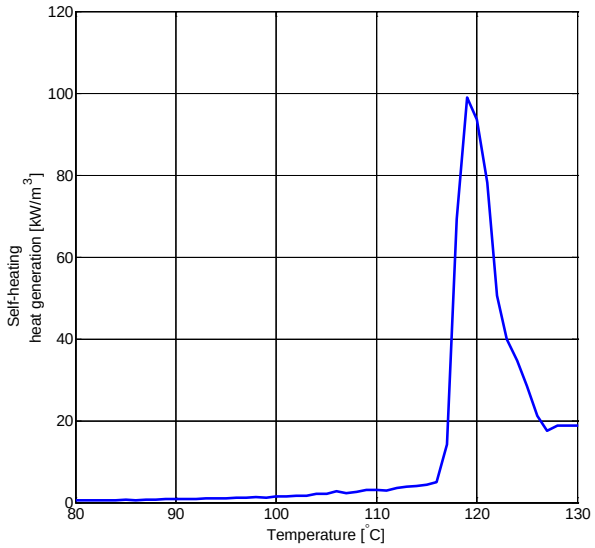

Figure 4 – Experimental self-heating curve implemented in the thermal model

CFD model

A 3D CFD model has the great advantage of providing detailed temperature and heat flux distribution within the battery module. The results allow for the identification of the presence of hot spots, understanding the time-dependent propagation of thermal waves within the pack as well as investigating the effect of resistive heating in localized portions of the module.

A finite volume model of the battery module has been developed in Star-CCM+.[7] The numerical model has been generated in order to account for the multi-layer structure of the pouch-cells resulting in a non-isotropic medium. The solution of the temperature distribution inside the cell was obtained by solving a three-dimensional conductive heat transfer equation in the cell domain:

$$\rho_c c_{p,c} \frac{\partial T}{\partial t} = \frac{\partial}{\partial x}\left(k_{ip} \frac{\partial T}{\partial x}\right) + \frac{\partial}{\partial y}\left(k_{ip} \frac{\partial T}{\partial y}\right) + \frac{\partial}{\partial z}\left(k_{op} \frac{\partial T}{\partial z}\right) + q + q_{sh} \qquad (2)$$

where *x a*nd *y* are the in-plane direction, *z* is the out of plane direction, and ρ_c and c_p are the average battery density and specific heat capacity, respectively. The two energy source terms, q and q_{sh}, represent the heat generations due to the normal battery operation and self-heating, respectively. A convective heat transfer was included in the model to account for the heat losses between the external wall and the environment. The ambient temperature was considered equal to 25°C.

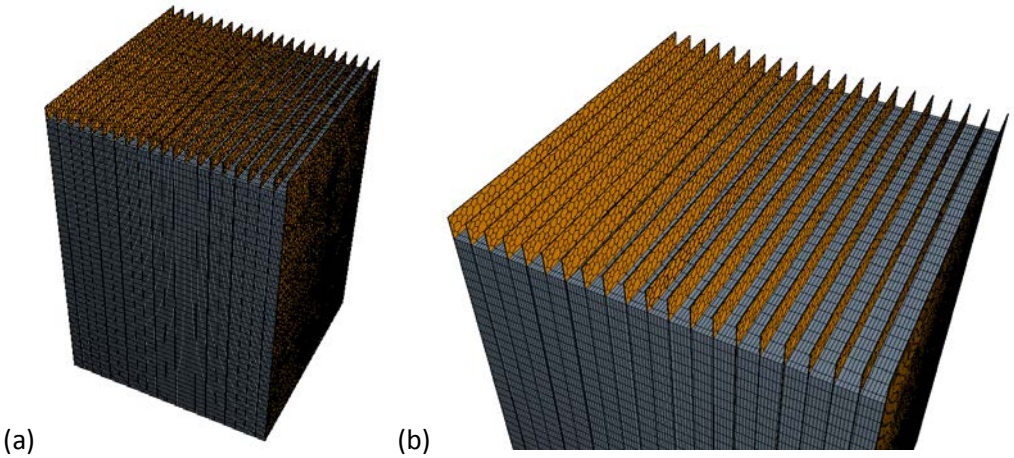

(a) (b)

Figure 5 – Three dimensional view of the mesh structure used in the CFD models.

The air in the gaps and the cooling channels were modelled using the classical Reynolds-averaged Navier-Stokes equations (RANS) complemented with the k-ε model for turbulence.[8]

Thermal model results

The CFD thermal model was used to simulate multiple layouts characterized by different cooling system operations. Table 3 summarizes all the layouts analyzed in the paper.

Table 3: summary of the scenarios analyzed			
	Cooling system type	**Cooling fluid**	**Coolant velocity [m/s]**
Layout 1	Natural convection	Air	-
Layout 2	Forced convection	Air	1
Layout 3	Forced convection	Air	2
Layout 4	Forced convection	Water	0.5

Figure 6 shows the steady state temperature contour on the battery cell external surface for each of the analyzed layouts. The results show that the core region of the module experiences temperatures that are about 2 to 3°C higher than the external region of the domain. The layered structure of the cell and the difference between in-plane and out-of-plane thermal conductivities result in a temperature field that is characterized by gradients that are larger in the out-of-plane direction in comparison to the in-plane direction. Nevertheless, the presence of the cooling fins produces a non-uniform temperature distribution across the cell planes. In particular, lower temperatures are observed in the upper portion of the module while the maximum temperature is reached on the bottom surface of the module.

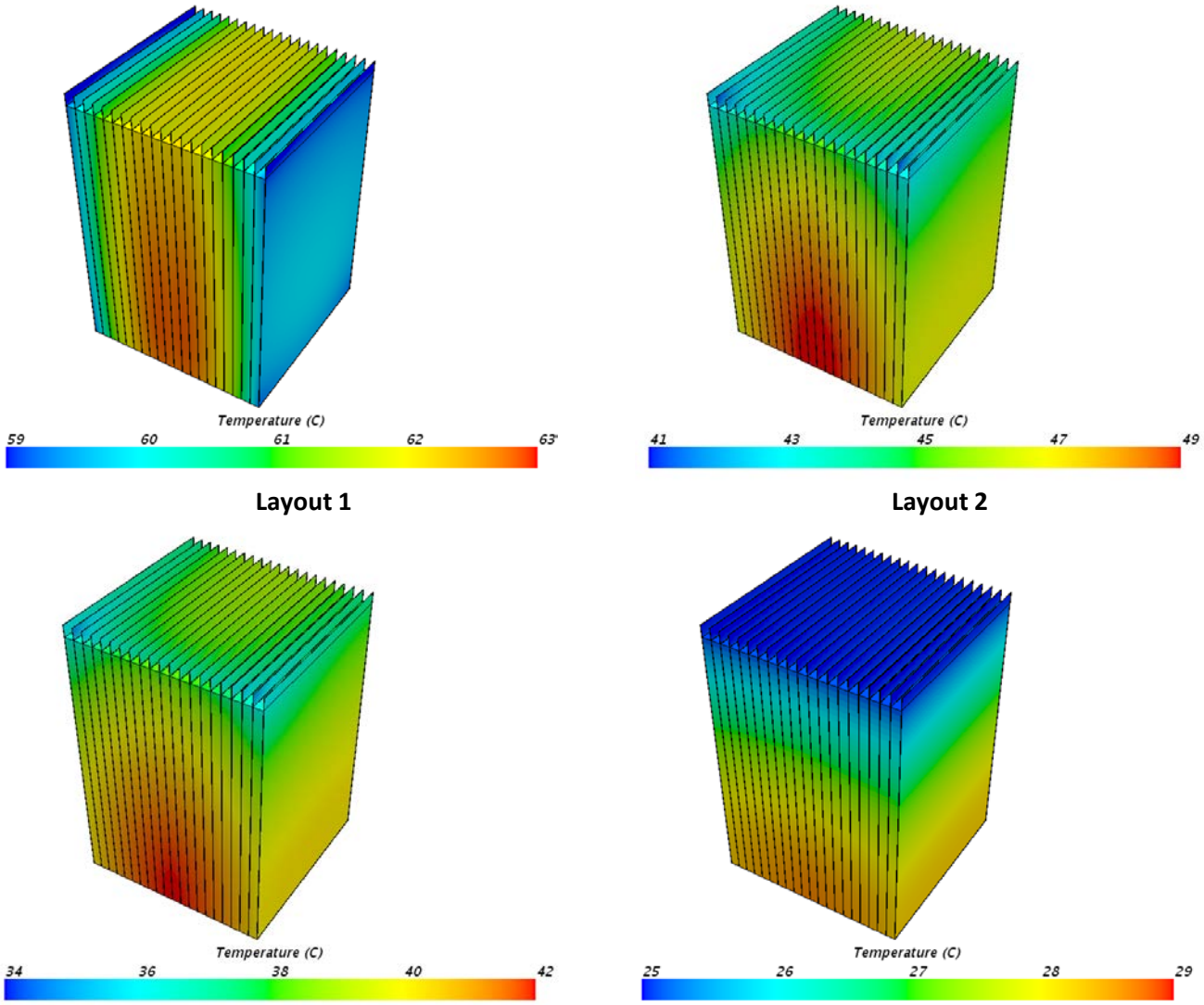

Layout 1 **Layout 2**

Layout 3 **Layout 4**

Figure 6 – Three dimensional view of the temperature distribution on the battery cells for layouts 1 to 4. Note that different temperature scales used for the temperature contours.

The comparative study shows the different effectiveness of the various thermal management system considered in this study. The maximum cell temperature was approximately equal to 63°C for layout 1 where natural convection is the only means of heat dissipation in the battery module.

An improvement in the heat removal is observed for layouts 2 and 3 where an air stream is used as a coolant. The maximum temperature is 49°C and 42°C for layouts 2 and 3, respectively. No appreciable effectiveness is observed for forced air velocities below 1 m/s. In addition, it should be noted that the heat removal is non-uniform across the battery pack due to the progressive increase in the coolant temperature as it flows through the cooling channels. This is confirmed by the local fin temperatures that tend to increase along the flow direction, being the lowest in the fluid inlet area. A marked improvement can be observed for layout 4. The larger mass flow rate of water as well as the increased film heat transfer coefficient associated with liquid results in an extremely effective removal of heat. In comparison to the previous layouts where the fin temperature approached the battery temperature, layout 4 is characterized by the fin temperature approaching the temperature of the coolant. This results in an extreme reduction of the temperature in the battery pack and in a very uniform removal of heat throughout the module. A summary of the average and maximum temperature in the battery modules is presented in Table 4.

Table 4: summary of the main results

	Average battery temperature [°C]	Maximum battery temperature [°C]
Layout 1	62	63
Layout 2	47	49
Layout 3	40	42
Layout 4	27	29

Figure 7 shows the temperature and velocity distribution across the cooling channels for layouts 2 and 4, respectively. Layout 2 is characterized by a progressively increasing air temperature due to the heat removal from the batteries through the metallic fins. This results in a non-uniform temperature distribution through the battery module and more effective cooling at the inlet side of the cooling channels. On the other hand, the water temperature distribution remains approximately constant through the channel due to the higher coolant mass flow rate, the large heat capacity of the water and the more effective heat transfer coefficient of the liquid. This results in very effective temperature control of the battery module.

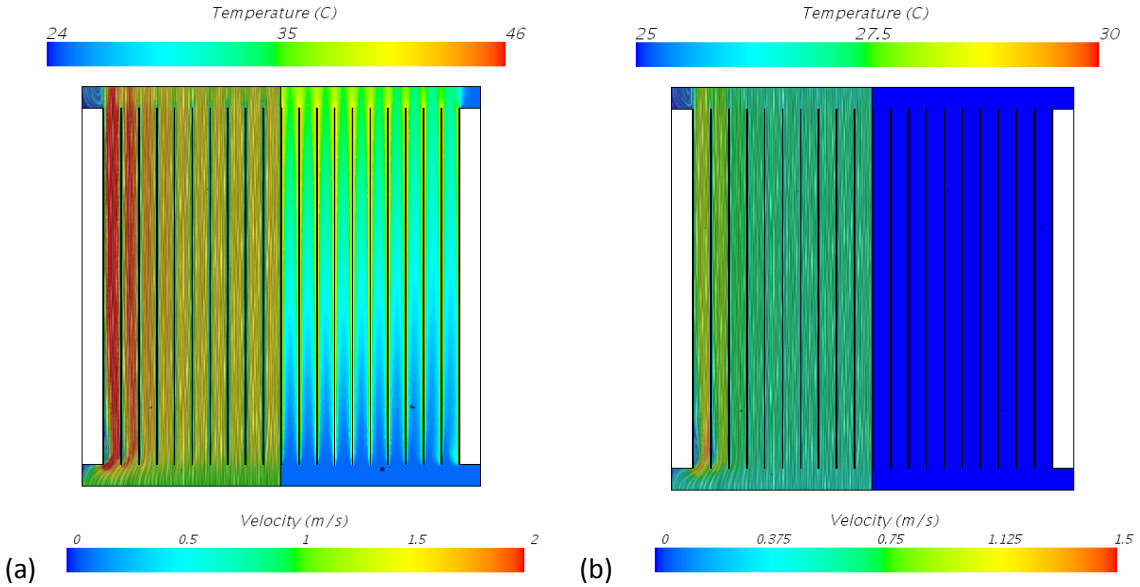

Figure 7 – Temperature and velocity distribution across the cooling channels for (a) Layout 2 and (b) Layout 4. Each figure displays velocity and temperature contours at the left and right hand side, respectively.

Conclusions

In this work, a framework for assessing the efficacy of a thermal management system is presented and discussed. In particular, the analysis combines experimental results and thermal modeling to assess the performance of thermal management systems for lithium-ion battery modules.

The lithium-ion cells were tested in an Accelerating Rate Calorimeter (ARC) in order to characterize the heat release rate associated with the initially slow exothermic reactions that are typically the precursor to a thermal runaway event. The test data were then used in a numerical model of a cell module. A CFD model was developed in Star-CCM+ to assess the effectiveness of thermal management systems.

Multiple layouts characterized by variable coolants (air and water) and natural or forced convection were used as benchmarks. The paper shows how computation fluid dynamics is a viable tool to simulate various thermal upset conditions and assess the performance of the thermal management systems. It allows for an effective comparison of different design alternatives including module operating conditions, coolant types and flow rates, fin dimensions and positioning, as well as the effectiveness of various thermal control algorithms. In addition, CFD models could be used for mapping different module operation regimes and to dynamically optimize the operation of heat removal systems to maximize performance.

References

1. Etacheri, V., et al. “Challenges in the development of advanced Li-ion batteries: a review.” Energy Environ. Sci., Vol. 4, pps. 3243-3263, 2011.
2. Fergus, J. “Recent developments in the cathode materials for lithium ion batteries.” J. Power Sources, Vol. 195, pps. 939-954, 2010.
3. Leising, R., et al. “Abuse Testing of Lithium-Ion Batteries.” J. Electrochem. Soc., Vol. 148, pps. A838-A844, 2001.
4. Townsend, D., “Thermal Hazard Evaluation by an Accelerating Rate Calorimeter.” Thermochimica Acta, Vol. 37, pps. 1-30, 1980.
5. Chen, S. C., Wan, C. C., Wang, Y.Y. (2005), “Thermal analysis of lithium-ion batteries”, Journal of Power Source (140): 111-124
6. Lindeburg, M.R. (2006), “Mechanical Engineering Reference Manual for the PE Exam. 12th edition”, Professional Publication, CA, USA.
7. CD-Adapco, Star-CCM+. V 7.04.011
8. Versteeg, H.K. and Malalasekera, W. (2007) “An introduction to computational fluid dynamics, the finite volume method (2nd ed)”, Pearson Prentice Hall, Glasgow.